

KINEMATICS ANALYSIS FOR HYBRID 2-(6-UPU) MANIPULATOR BY WAVELET NEURAL NETWORK

Arash Rahmani^{1*}, Ahmad Ghanbari^{1,2}, Mehran Mahboubkhah¹

¹ Department of Mechanical Engineering, University of Tabriz, Tabriz, Iran.

² School of Engineering Emerging Technologies, Mechatronics Laboratory, University of Tabriz, Tabriz, Iran.

*Corresponding author Email: ara_rahmani@yahoo.com

ABSTRACT: *This paper presents forward and inverse Kinematics analysis of a specific class of series-parallel manipulators, known as 2(6-UPU) manipulators, which composed of two modules which consist of elementary manipulators with the parallel structure of the Stewart Platform. At first, the Kinematics Model of the hybrid manipulator is obtained. Then, As Inverse kinematics problem of this kind of manipulators is a very difficult problem to solve because of their highly nonlinear relations between joint variables and position and orientation of the end effectors. Therefore, wavelet based neural network (wave-net) with its inherent learning ability as a strong method, was used to solve the inverse kinematics problem. Also, proposed wavelet neural network (WNN) is applied to approximate the paths of mid and upper plate in circle and spiral path respectively. The results show high accurate performance of proposed WNN.*

Key words: *Hybrid Manipulators, Kinematics Analysis, Network Training, Nonlinear System, Neural, Network, Wavelet*

1. INTRODUCTION

A hybrid manipulation system is a sequence of parallel mechanisms which can overcome the limited workspace of parallel mechanism and can provide feature of both serial and parallel mechanism. They are able to achieve high stiffness and high force-to-weight ratio. The hybrid serial-parallel robotic manipulator has attracted the attention of many researchers and it also has growing applications to robotics, machine tools, positioning systems, measurement devices, and so on. It has been proved great potential and advantage both closed-loop and opened-loop manipulator over the traditional manipulator. Many different types of hybrid robots have been investigated [1,2,3]. Tanev [4] presented a hybrid (parallel serial) manipulator consisting of two serially connected parallel mechanisms and overall 6DOF and gave its closed-form solution for forward and inverse position problems. Romdhane [5] investigated the hybrid manipulator which made of a base and two platforms in series and the motion of the mid platform is restricted only to three translations and the second platform rotates spherically with respect to the mid platform using joint connected the mid platform and top platform. The characteristics of 6 DOF parallel-serial hybrid manipulators which features a 3 DOF in series actuated module mounted on the moving plate of another 3 DOF in parallel actuated manipulator with prismatic actuators is studied in [6]. The kinematics of hybrid type manipulation system with 6 DOF, which consist of a 3-DOF planar parallel platform and a 3-DOF serial robot arm, is discussed by Yang et al. [7]. Huang et al. [8] studied a conceptual design and dimensional synthesis of a 3-DOF parallel mechanism module which forms the main body of a newly invented 5-DOF reconfigurable hybrid robot. LiangZhi et al. [9] studied a hybrid 5DOF manipulator based on the novel 3-RPS inactuated parallel manipulator. In their design a 2DOF serial working table is placed over the mobile platform. A new methodology to synthesize hybrid robots as a whole structure is presented by Campos et al. [10]. Their method is based on Assure groups as the simplest basic blocks to build

kinematic chains. Gallardo et al. [11] studied Kinematics and dynamics of 2(3-RPS) manipulators by means of screw theory and the principle of virtual work. A novel 3RPS-3SPR serial-parallel manipulator (S-PM) with 6 degree of freedoms is proposed in [12] and its inverse kinematics, active forces and workspace are solved. First, the inverse displacement is solved in close form based on the geometrical and the dimensional constraints then, Jacobian matrices are derived and the active forces are solved using principle of virtual work. Gallardo et al. [13] address the kinematics, including position, velocity and acceleration analyses, of a modular spatial hyper-redundant manipulator built with a variable number of serially connected identical mechanical modules with autonomous motions. Li et al. [14] used a hybrid manipulator as a multi-dimensional vibration isolator based on the parallel mechanism. The scheme design, inverse kinematics, workspace and dexterity are carried out in their paper. Kizir et al. [15] used Kane transition function to generate several trajectories for controlling a high precision hybrid platform by a PID and sliding mode controller. Chen et al. [16] proposed a multi-objective genetic algorithm trajectory planner for a PKM, based on the dynamics approach. Ghanbari et al. [17] present neural network solution for forward kinematic of a novel hybrid mechanism which composed a sequence of two Stewart platforms mechanisms.

In this paper a novel hybrid robot 2(6-UPU) is introduced that composed a sequence of two same Stewart mechanism modules. The serial form of these hybrid manipulators overcomes the limited workspace of parallel manipulators and improves overall stiffness and response characteristics. Then, kinematic model of the hybrid robot is presented and Because of their highly nonlinear relations between joint variables and position and orientation of the end effectors, wavelet neural network has been provided and used to solve the inverse kinematics. Also, proposed WNN is applied to approximate the paths of mid and upper plate in circle and spiral path respectively.

2. DESCRIPTION OF THE HYBRID ROBOT

The mechanism under investigation in this paper consists of two same modules that each module is Stewart Platform mechanism with 6 DOFs. In this hybrid mechanism, we have three platforms and twelve pods. Base platform is stationary and connected to middle platform via 6 extensible pods. Also, middle platform is connected to upper platform (as an end effector) via 6 extensible pods. Each pod connects to the platform at its connection point through a universal joint, and to the base at its connection point through universal joint too. Each pod consists of two parts: the upper part and the lower part, which connect to each other through prismatic joint. Therefore, it is referred to as the 2 (6-UPU) mechanisms. This manipulator is actuated by motors located on the prismatic joints. Figure 1 shows the design of the mentioned hybrid robot.

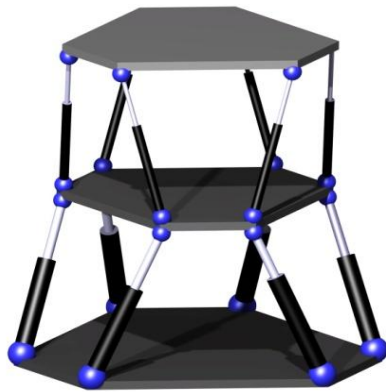


Fig.1. Schematic for 2(6-UPS) hybrid robot

3. FORWARD AND INVERSE KINEMATICS SOLUTION

Mechanism kinematics deals with the study of the mechanism motion as constrained by the geometry of the links. Typically, the study of mechanism kinematics is divided into two parts: inverse kinematics and direct kinematics. About mentioned hybrid robot, the inverse kinematics problem involves mapping a known pose (position and orientation) of the moving platforms of the mechanism to a length of each module's pods. The direct kinematics problem involves the mapping from a known length of each module's pods to a pose of the moving platforms. In this section the inverse and forward kinematics problems of proposed mechanism are described in closed form.

Figure 2 shows the vectorial representation of the i^{th} pod at each module. According to fig. 2, the middle and upper moving platforms frame are shown by {C} and {C'} respectively and base frame with {O}. Also,

$$P^m = (x^m, y^m, z^m, \alpha^m, \beta^m, \gamma^m) \text{ and}$$

$P^u = (x^u, y^u, z^u, \alpha^u, \beta^u, \gamma^u)$ present the location (position and orientation) of the middle and upper moving platform respectively. Now, the inverse kinematics of each module is

obtained at first, and then forward kinematics is considered. Inverse Kinematic problem of the platforms involves determination of the linear position, of six Pods for each module through considering a specified position, of the middle and upper moving platforms centre.

A. Middle Moving Platform

The length vector of the i^{th} pod in the base module can be obtained as:

$$\vec{L}_i = \vec{op}_i - \vec{b}_i \quad \text{for } i = 1, 2, \dots, 6 \quad (1)$$

$$\vec{op}_i = \vec{D}_i + (R \cdot \vec{cp}_i) \quad (2)$$

Where R is the rotation 3x3 matrix, representing the rotation of frame {C} related to frame {O} and it is defined if

$P^m = (x^m, y^m, z^m, \alpha^m, \beta^m, \gamma^m)$ is obvious:

$$R = \begin{bmatrix} R_{11} & R_{12} & R_{13} \\ R_{21} & R_{22} & R_{23} \\ R_{31} & R_{32} & R_{33} \end{bmatrix} \quad (3)$$

Also,

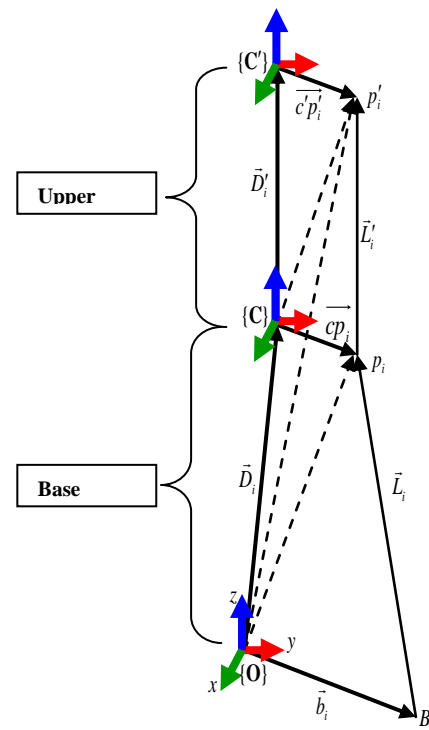


Fig.2. vectorial representation of the i^{th} pod at each module

$$\vec{D}_i = \vec{D} = \begin{bmatrix} D_x \\ D_y \\ D_z \end{bmatrix}, \quad \vec{b}_i = \begin{bmatrix} b_{xi} \\ b_{yi} \\ b_{zi} \end{bmatrix}, \quad \vec{cp}_i = \begin{bmatrix} p_{xi} \\ p_{yi} \\ p_{zi} \end{bmatrix} \quad (4)$$

Using equation (1) to (4), the length of the i^{th} pod, L_i , for base module can be expressed as:

$$\vec{L}_i = \begin{bmatrix} L_{xi} \\ L_{yi} \\ L_{zi} \end{bmatrix} = \begin{bmatrix} D_x + R_{11}p_{xi} + R_{12}p_{yi} + R_{13}p_{zi} - b_{xi} \\ D_y + R_{21}p_{xi} + R_{22}p_{yi} + R_{23}p_{zi} - b_{yi} \\ D_z + R_{31}p_{xi} + R_{32}p_{yi} + R_{33}p_{zi} - b_{zi} \end{bmatrix} \quad (5)$$

$$L_i = \sqrt{L_{xi}^2 + L_{yi}^2 + L_{zi}^2} \quad (6)$$

B. Upper Moving Platform

The length vector of the i^{th} pod in the upper module can be obtained as:

$$\vec{L}'_i = \vec{op}'_i - \vec{op}_i \quad \text{for } i=1,2,\dots,6 \quad (7)$$

Where:

$$\vec{op}'_i = \vec{D}_i + R \cdot \vec{D}'_i + RR' \cdot \vec{c}'p'_i \quad \text{for } i=1,2,\dots,6 \quad (8)$$

By substituting Eqs (2) and (8) into Eq. (7) And considering:

$$H = RR' = \begin{bmatrix} H_{11} & H_{12} & H_{13} \\ H_{21} & H_{22} & H_{23} \\ H_{13} & H_{23} & H_{33} \end{bmatrix} \quad (9)$$

And:

$$\vec{D}'_i = \vec{D}' = \begin{bmatrix} D'_x \\ D'_y \\ D'_z \end{bmatrix}, \quad \vec{c}'p'_i = \begin{bmatrix} p'_{xi} \\ p'_{yi} \\ p'_{zi} \end{bmatrix}$$

L'_i can be expressed as:

$$\vec{L}'_i = \begin{bmatrix} L'_{xi} \\ L'_{yi} \\ L'_{zi} \end{bmatrix} = \begin{bmatrix} R_{11}D'_x + R_{12}D'_y + R_{13}D'_z + H_{11}p'_{xi} + H_{12}p'_{yi} + H_{13}p'_{zi} - R_{11}p_{xi} - R_{12}p_{yi} - R_{13}p_{zi} \\ R_{21}D'_x + R_{22}D'_y + R_{23}D'_z + H_{21}p'_{xi} + H_{22}p'_{yi} + H_{23}p'_{zi} - R_{21}p_{xi} - R_{22}p_{yi} - R_{23}p_{zi} \\ R_{31}D'_x + R_{32}D'_y + R_{33}D'_z + H_{31}p'_{xi} + H_{32}p'_{yi} + H_{33}p'_{zi} - R_{31}p_{xi} - R_{32}p_{yi} - R_{33}p_{zi} \end{bmatrix}$$

$$L'_i = \sqrt{L'_{xi}^2 + L'_{yi}^2 + L'_{zi}^2} \quad (12)$$

After Inverse Kinematics analysis of 2(6-UPU), we want to calculate the location and orientation of the middle and upper moving platform by knowing the length of pods at each module (Forward Kinematics). As, it is clear, we can rewrite equations (1) and (7) as below:

$$f_i(X) = \vec{D}_i + R \cdot \vec{cp}_i - \vec{b}_i - \vec{L}_i = 0 \quad (13)$$

$$g_i(X') = R \cdot \vec{D}'_i + H \cdot \vec{c}'p'_i - R \cdot \vec{cp}_i - \vec{L}'_i = 0 \quad (14)$$

The solution of above equations is the kinematics problem of the mechanisms. But, because of highly nonlinear characteristic of these equations, it is so difficult to solve them in direct kinematics form. Therefore, wavelet based neural network (wave-net) is applied to solve forward kinematics of this mechanism.

4. Wavelet Neural Network
4-1 Structure of network

The wavelet neural network (WNN) is the model based on wavelet transformation and artificial neural network [18]. Due to wavelet transform has the good localization characteristics in time and frequency domain and neural networks has the good ability to approximate complicated maps, WNN incorporate the good learning ability and the good property of localization, which have been successfully applied in function approximation and pattern classification. A neural network is constructed by interconnecting a number of neurons so as to form a network in which all connections are made in the forward direction.

Because the approximation class is nonlinear in the adjustable parameters, the training procedure of the neural networks may become trapped in some local minimum depending on the initialization. To overcome this problem, the wavelet networks have been proposed as an alternative to neural networks, which follow the availability of rates of convergence for approximation by wavelet based networks. In this section a feed forward single hidden layer network is introduced. For a (back propagation) BP neural network with only one hidden layer of neurons, using basis wavelets as its activate functions of hidden layer, we get a multi-input and multi-output wavelet neural networks in Fig. 3.

This WNN has m, p, n nodes in the input layer, hidden layer and output layer respectively. And the activate function of the j^{th} node in the hidden layer is [19]:

$$\psi_{a_j, b_j}(t) = \frac{1}{\sqrt{a_j}} \psi\left(\frac{t - b_j}{a_j}\right) \quad j = 1, 2, \dots, p \quad (15)$$

Where, $\psi(t)$ is the mother wavelet function which is localized both in time and frequency and could be chosen as different function according to the feature of the problem? Fig. 4 shows four types of most applicable wavelet functions. In this paper we use Mexican Hat wavelet. This wavelet is derived from a function, which is proportional to the second derivative function of the Gaussian probability density function. It is non-orthogonal, with infinite support and has maximum energy around origin with the narrow band. The expression for Mexican Hat wavelet is given by Eq. (16). In this paper, $f(t)$ is chosen as sigmoid function.

$$\psi(t) = (1 - 2t^2) \cdot \exp(-t^2) \quad (16)$$

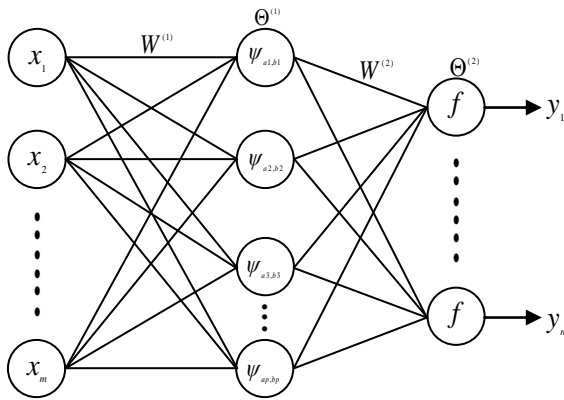


Fig.3. Structure of WNN

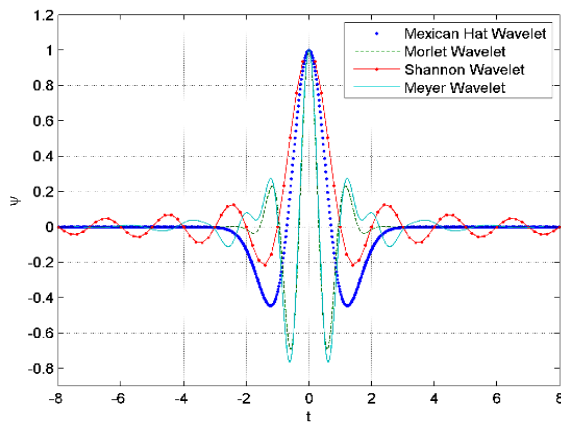


Fig.4. Wavelet Functions

The wavelet neural network parameters in Fig. 3, $(W^{(1)}, W^{(2)}, \Theta^{(1)}, \Theta^{(2)}, a_1, \dots, a_p, b_1, \dots, b_p)$, should be adjusted through training.

4-2 Training of network

Back propagation method is the most frequently used technique for training a feed forward network. It involves two passes through the network, a forward pass and a backward pass. The forward pass generates the network's output activities and the backward pass involves propagating the error initially found in the output nodes back through the network to assign errors to each node that contributed to the initial error. Once all the errors are assigned, the weights are changed so as to minimize these errors. Since the WNN in Fig. 3 is derived from a feed forward neural network, we use back propagation method to train this network. For the WNN in Fig. 3, when the input vector is $\mathbf{X} = (x_1, x_2, \dots, x_m)$, we get the output of the j^{th} node in hidden layer:

$$\psi_{a_j, b_j} \left(\sum_{k=1}^m w_{jk}^{(1)} x_k - \theta_j^{(1)} \right) = \psi_{a_j, b_j} (F_j^{(1)}) = \frac{1}{\sqrt{a_j}} \psi \left(\frac{F_j^{(1)} - b_j}{a_j} \right) \tag{17}$$

Where,

$$F_j^{(1)} = \sum_{k=1}^m w_{jk}^{(1)} x_k - \theta_j^{(1)} \tag{18}$$

the output of the i^{th} node of output layer is:

$$y_i = f \left(\sum_{j=1}^p w_{ij}^{(2)} \psi_{a_j, b_j} (F_j^{(1)}) - \theta_i^{(2)} \right) = f (F_i^{(2)}) \tag{19}$$

Where,

$$F_i^{(2)} = \sum_{j=1}^p w_{ij}^{(2)} \psi_{a_j, b_j} (F_j^{(1)}) - \theta_i^{(2)} \tag{20}$$

From equation (19) we get the output vector of the WNN: $\mathbf{Y} = (y_1, y_2, \dots, y_n)$. Suppose we have Q training samples. For each sample q , the desired output vector is $\bar{\mathbf{Y}}_q = (\bar{y}_{q1}, \bar{y}_{q2}, \dots, \bar{y}_{qn})$, the output vector of the WNN is $\mathbf{Y}_q = (y_{q1}, y_{q2}, \dots, y_{qn})$. With these Q training samples, we train the WNN through batch learning process. Then the main goal of the network is to minimize the total error E of each output node i over all training samples [21]:

$$E = \frac{1}{2} \sum_{q=1}^Q \sum_{i=1}^n (\bar{Y}_{qi} - Y_{qi})^2 \tag{21}$$

By the iterative gradient descent method, the parameters of the wavelet neural network can be formulated by:

$$w_{ij}^{(2)}(t+1) = (1 + \beta)w_{ij}^{(2)}(t) - \beta w_{ij}^{(2)}(t-1) - \lambda \frac{\partial E}{\partial w_{ij}^{(2)}} \tag{22}$$

$$w_{jk}^{(1)}(t+1) = (1 + \beta)w_{jk}^{(1)}(t) - \beta w_{jk}^{(1)}(t-1) - \lambda \frac{\partial E}{\partial w_{jk}^{(1)}} \tag{23}$$

$$\theta_i^{(2)}(t+1) = (1 + \beta)\theta_i^{(2)}(t) - \beta \theta_i^{(2)}(t-1) - \lambda \frac{\partial E}{\partial \theta_i^{(2)}} \tag{24}$$

$$\theta_j^{(1)}(t+1) = (1 + \beta)\theta_j^{(1)}(t) - \beta \theta_j^{(1)}(t-1) - \lambda \frac{\partial E}{\partial \theta_j^{(1)}} \tag{25}$$

$$a_j(t+1) = (1 + \beta)a_j(t) - \beta a_j(t-1) - \lambda \frac{\partial E}{\partial a_j} \tag{26}$$

$$b_j(t+1) = (1 + \beta)b_j(t) - \beta b_j(t-1) - \lambda \frac{\partial E}{\partial b_j} \tag{27}$$

Where t is the iteration index of learning and λ is the learning rate. To improve the rate of learning, we modify the original learning rule with the momentum factor β ($0 < \beta < 1$) to the weights [20]. The partial derivatives of the error E respect to each parameter can be calculated easily.

5. WNN solution for Kinematics of Robot

In order to model forward Kinematics of hybrid robot with wave-net, according to structure of robot. We have modeled the base module and the upper, respectively. The input data of the network are the length of pods for each module. At first, using the length of pods of the base module, $\mathbf{L}^b = (l_1^b, l_2^b, l_3^b, l_4^b, l_5^b, l_6^b)$, we define the position and orientation of the middle plate, $P^m = (x^m, y^m, z^m, \alpha^m, \beta^m, \gamma^m)$. Then, using the length of pods of the upper module, $\mathbf{L}^u = (l_1^u, l_2^u, l_3^u, l_4^u, l_5^u, l_6^u)$, and the position and orientation of the middle plate, we calculated the position and orientation of the upper plate(end effector), $P^u = (x^u, y^u, z^u, \alpha^u, \beta^u, \gamma^u)$. Therefore, we have two different networks.

The algorithm of wavelet neural network for approximate the kinematics of hybrid robot is summarized as follows:

Step 1: Set the initial values of networks parameters ($W^{(1)}, W^{(2)}, \Theta^{(1)}, \Theta^{(2)}, a_1, \dots, a_p, b_1, \dots, b_p$), learning rate λ and momentum factor β .

Step 2: Input the training data and the desired output values. Give input vectors $\mathbf{X} = (x_1, x_2, \dots, x_m)$ where it is the length of pods of each module and a desired output vector $\bar{\mathbf{Y}}_q = (\bar{y}_{q1}, \bar{y}_{q2}, \dots, \bar{y}_{qn})$, the theoretical values acquired from inverse kinematic solution of Eqs. (13) and (14).

Step 3: For each input datum, calculate the output of the wavelet neural network by Eq. (19).

Step 4: Adjust the networks parameters ($W^{(1)}, W^{(2)}, \Theta^{(1)}, \Theta^{(2)}, a_1, \dots, a_p, b_1, \dots, b_p$) using gradient descent algorithm by Eq. (22) to (27).

Step 5: The error function E is calculated by Eq. (21). If the error is less than the desired bound, the networks parameters

are obtained and the learning process is terminated, else go to step2.

6. RESULTS

In this section, we present the results of the proposed WNN on approximating the kinematic analysis of hybrid robot. The architecture was used for the wavelet network is one input layer with six neurons, one hidden layer with 64 neurons and one output layer with six neurons. The network was trained with a learning rate of 0.15, a momentum term of 0.1, and 1,024 learning iterations. The largest error E or given precision is %1.5. Table 1 shows sample results of direct kinematics with reference length of pods ($L_0 = 550\text{mm}$) and pods length variation of base module and upper module:

$$\mathbf{L}_{Base} = (l_1 = 240\text{mm}, l_2 = 50\text{mm}, l_3 = 110\text{mm}, l_4 = 190\text{mm}, l_5 = 230\text{mm}, l_6 = 300\text{mm})$$

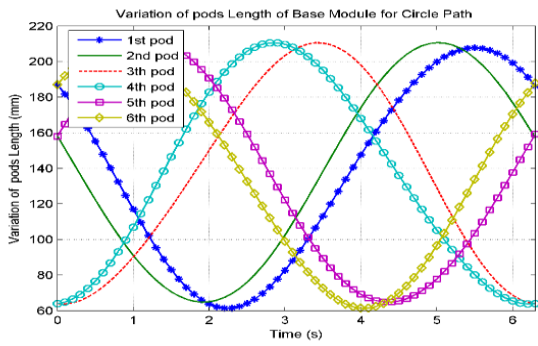
$$\mathbf{L}_{Upper} = (l_1 = 210\text{mm}, l_2 = 140\text{mm}, l_3 = 290\text{mm}, l_4 = 260\text{mm}, l_5 = 120\text{mm}, l_6 = 40\text{mm})$$

And comparison of WNN with closed form solutions (CFS).

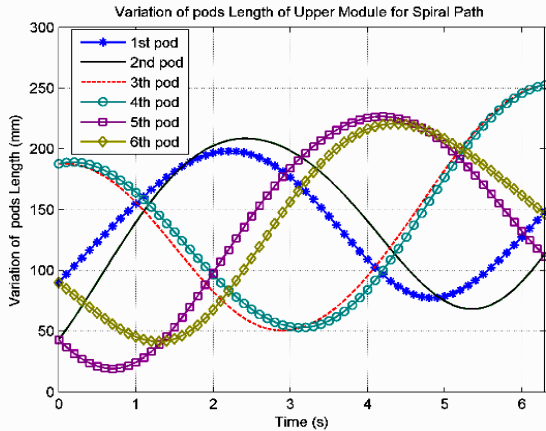
Also, figures 5 to 8 show the results of the proposed WNN for the specific paths of middle and upper plates of hybrid robot. Results given here are for circle path and spiral path with elliptical base curve for center point of middle and upper plate, respectively. Using inverse kinematic analysis for proposed paths of plates, we define motions of each pod of each module (figures 5). Then, we feed the proposed WNN by the pods motions to get the paths of plates. Figure 6 shows the position paths and figure 7 shows orientation paths for center point of each plate. Again, we used the outputs of the proposed WNN for inverse kinematic analysis to define the new motions of each pod of each module and compared them with the pods motions which results from CFS. Figure 8 show the results, for variation of length of each pods of base and upper module for circle path for center point of mid plate with $(10 \times [-\cos t^\circ, \sin t^\circ, 0^\circ])$ orientation and spiral path with elliptical base curve for center point of upper plate with $(10 \times [\cos t^\circ, -\sin t^\circ, 0^\circ])$ orientation.

Table. 1: Results of CFS and WNN for a sample case of each pods length variation for each module

Base Module (L1=240 mm, L2=50 mm, L3=110 mm, L4=190 mm, L5=230 mm, L6=300 mm)												
mid Plt.	x (mm)		y (mm)		z (mm)		alfa (deg)		beta (deg)		gama (deg)	
	CFS	WNN	CFS	WNN	CFS	WNN	CFS	WNN	CFS	WNN	CFS	WNN
	28.972	28.616	48.009	48.211	62.768	63.371	-12.612	-12.440	12.329	12.412	0.796	0.792
% Err	-1.23%		0.42%		0.96%		-1.36%		0.67%		-0.46%	
Upper Module (L1=210 mm, L2=140 mm, L3=290 mm, L4=260 mm, L5=120 mm, L6=40 mm)												
Upper Plt.	x (mm)		y (mm)		z (mm)		alfa (deg)		beta (deg)		gama (deg)	
	CFS	WNN	CFS	WNN	CFS	WNN	CFS	WNN	CFS	WNN	CFS	WNN
	63.537	61.745	51.997	52.652	78.259	76.318	15.254	15.702	-2.732	-2.812	8.098	7.887
% Err	-2.82%		1.26%		-2.48%		2.94%		2.93%		-2.60%	

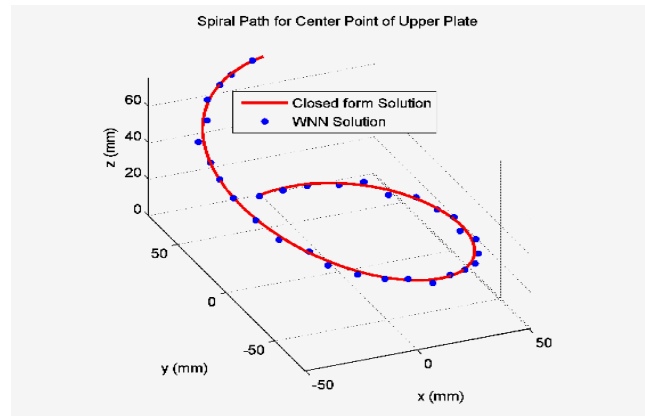


(a)



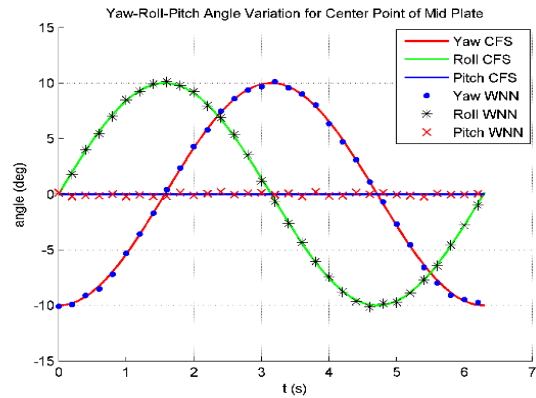
(b)

Fig.5: (a) Variation of length of pods of base module for circle path with Orientation $(10 \times [-\cos t^\circ, \sin t^\circ, 0^\circ])$
 (b) Variation of length of pods of upper module for spiral path with Orientation $(10 \times [\cos t^\circ, -\sin t^\circ, 0^\circ])$

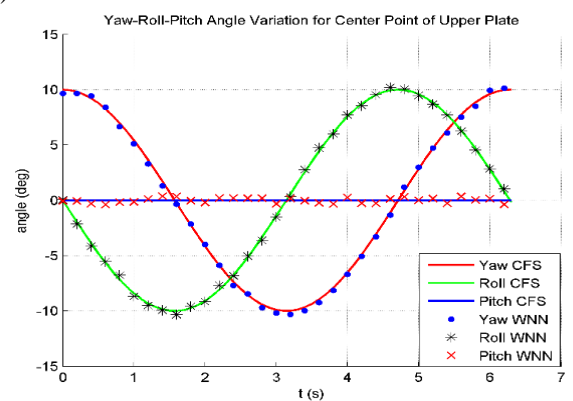


(b)

Fig.6: (a) Circle Path for Center Point of Mid Plate with Orientation $(10 \times [-\cos t^\circ, \sin t^\circ, 0^\circ])$
 (b) Spiral Path for Center Point of Upper Plate with Orientation $(10 \times [\cos t^\circ, -\sin t^\circ, 0^\circ])$

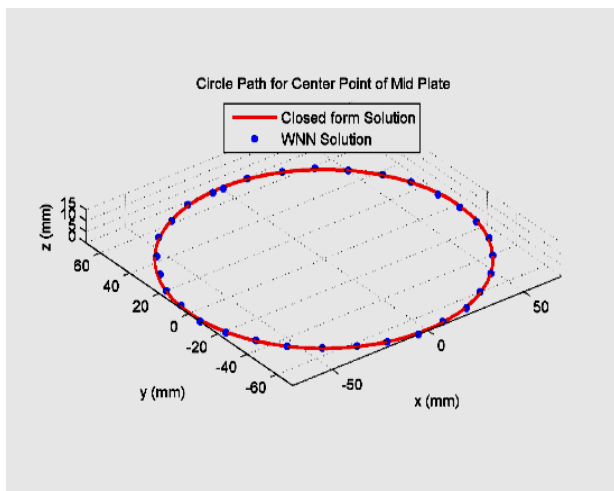


(a)



(b)

Fig.7: (a) Orientation Path for Center Point of Mid Plate
 (b) Orientation Path for Center Point of Upper Plate



(a)

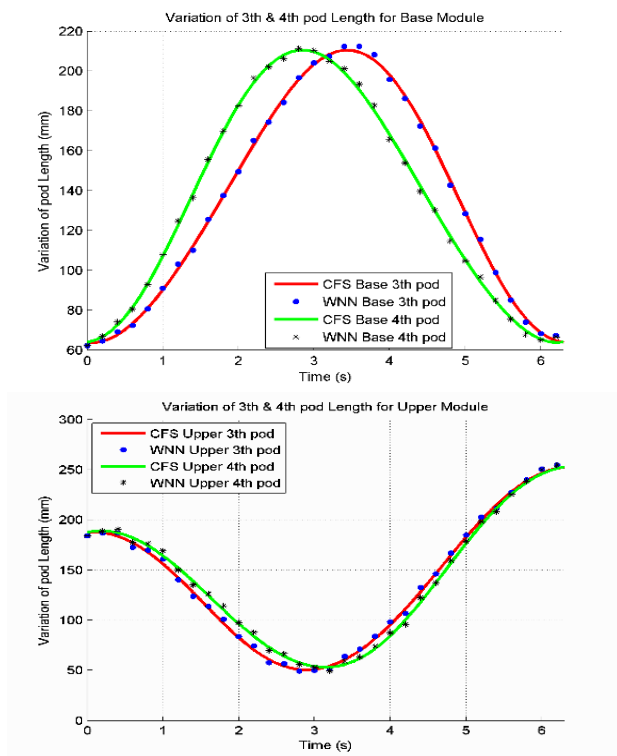
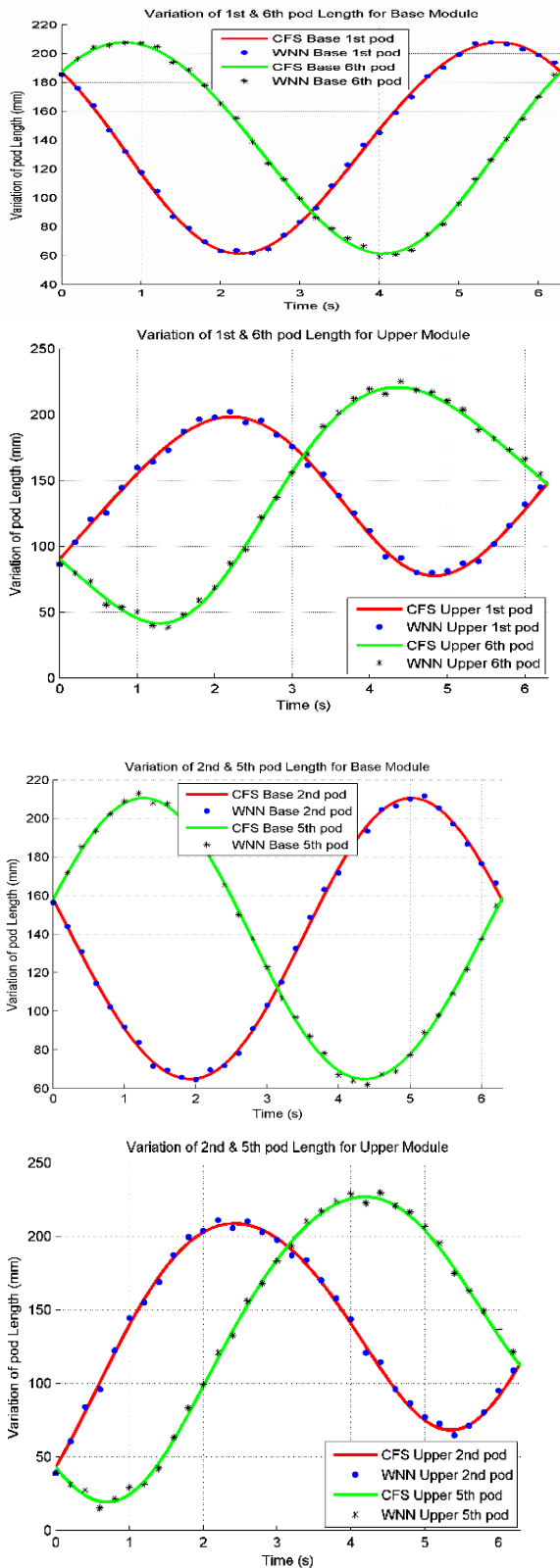


Fig.8: Length Variation of pods of base and upper module for

circle and spiral path respectively with defined orientation change. The results show good agreement between exact solution (CFS) and outputs of proposed WNN. Although, the accumulation of error for kinematic analysis of upper module, causes the error percentage in results of upper plate position and orientation is higher than mid plate. Accumulation of error for kinematic analysis of upper module is derived:

- 1- Network error
- 2- Input error (the outputs of WNN for base module with error, are also fixed inputs for WNN for upper plates).

6. CONCLUSIONS

In this paper, a wavelet neural network, which can be employed as a useful tool for nonlinear mapping problem has been proposed for solving direct kinematics of hybrid robot. The proposed network can be proved to have the capability of approximating any multivariable systems. Whereas, the kinematics model of hybrid robot has strongly nonlinear characteristic, the network can not only be trained in a short time, but also shows better performance in solving problems. According to the results, there is good agreement between WNN and CFS, but, because of accumulation of error, the error of results of upper plate is more than the error of the mid plate. Although, according networks tanning approach the maximum error for all cases is less than 1.5%.

7. REFERENCES:

1. Carbone, G., & Ceccarelli, M., "A stiffness analysis for a hybrid parallel-serial manipulator". *Robotica*, **22**(5): 567-576 (2004).
2. Rico, J., Gallardo, J., & Duffy, J., "Screw theory and higher order kinematic analysis of open serial and closed chains". *Mechanism and Machine Theory*, **34**(4): 559-586 (1999).
3. Zhou, B., & Xu, Y., "Robust control of a 3-DOF hybrid robot manipulator". *The International Journal of Advanced Manufacturing Technology*, **33**(5-6): 604-613 (2007).
4. Tanev, T. K., "Kinematics of a hybrid (parallel-serial) robot manipulator". *Mechanism and Machine Theory*, **35**(9): 1183-1196 (2000)
5. Romdhane, L., "Design and analysis of a hybrid serial-parallel manipulator". *Mechanism and Machine Theory*, **34**(7): 1037-1055(1999).
6. Huang, M. Z., Ling, S.-H., & Sheng, Y., "A study of velocity kinematics for hybrid manipulators with parallel-series configurations". *Paper presented at the Robotics and Automation, Proceedings., 1993 IEEE International Conference on* (1993).
7. Yang, G., Chen, W., & Ho, E. H. L., "Design and kinematic analysis of a modular hybrid parallel-serial manipulator". *Paper presented at the Control, Automation, Robotics and Vision, 2002. ICARCV 2002. 7th International Conference on* (2002).
8. Huang, T., Li, M., Zhao, X., Mei, J., Chetwynd, D. G., & Hu, S. J., "Conceptual design and dimensional synthesis for a 3-DOF module of the TriVariant-a novel 5-DOF reconfigurable hybrid robot". *Robotics, IEEE Transactions on*, **21**(3): 449-456(2005).
9. LiangZhi, F., Elatta, A., & XiaoPing, L., "Kinematic calibration for a hybrid 5DOF manipulator based on 3-RPS in-actuated parallel manipulator". *The International Journal of Advanced Manufacturing Technology*, **25**(7-8): 730-734 (2005).
10. Campos, A., Budde, C., & Hesselbach, J. A., "type synthesis method for hybrid robot structures". *Mechanism and Machine Theory*, **43**(8): 984-995(2008).
11. Gallardo-Alvarado, J., Aguilar-Nájera, C. R., Casique-Rosas, L., Rico-Martínez, J. M., & Islam, M. N., "Kinematics and dynamics of 2 (3-RPS) manipulators by means of screw theory and the principle of virtual work". *Mechanism and Machine Theory*, **43**(10): 1281-1294 (2008).
12. Hu, B., Lu, Y., Yu, J. J., & Zhuang, S., "Analyses of Inverse Kinematics, Statics and Workspace of a Novel 3RPS-3SPR Serial-Parallel Manipulator". *The Open Mechanical Engineering Journal*, **5**: 65-72 (2012).
13. Gallardo, J., Lesso, R., Rico, J. M., & Alici, G., "The kinematics of modular spatial hyper-redundant manipulators formed from RPS-type limbs". *Robotics and Autonomous Systems*, **59**(1): 12-21 (2011).
14. Li, B., Zhao, W., & Deng, Z., "Modeling and analysis of a multi-dimensional vibration isolator based on the parallel mechanism". *Journal of Manufacturing Systems*, **31**(1): 50-58(2012).
15. Kizir, S., & Bingul, Z. (Eds.), "Position Control and Trajectory Tracking of the Stewart Platform": InTech (2012).
16. Chen, C.-T., & Pham, H.-V., "Trajectory planning in parallel kinematic manipulators using a constrained multi-objective evolutionary algorithm". *Nonlinear Dynamics*, **67**(2): 1669-1681(2012).
17. Ghanbari, A., & Rahmani, A., "Neural network solutions for forward kinematics problem of hybrid serial-parallel manipulator". *World of Sciences Journal*, **1**(8): 148-158 (2013).
18. Zhang, Q., & Benveniste, A., "Wavelet networks". *Neural Networks, IEEE Transactions on*, **3**(6): 889-898 (1992).
19. Banakar, A., & Azeem, M. F., "Artificial wavelet neuro-fuzzy model based on parallel wavelet network and neural network". *Soft Computing*, **12**(8): 789-808 (2008).
20. Chen, D., & Han, J., "Application of wavelet neural network in signal processing of MEMS accelerometers". *Microsystem technologies*, **17**(1): 1-5(2011).
21. Huang, M., & Cui, B., "A novel learning algorithm for wavelet neural networks" *Advances in Natural Computation* (pp. 1-7): Springer (2005).